






Wavelet-Based Spatial Resolution Enhancement for Thermal Images

Wasnaa Witwit^{1*}, Yifan Zhao², Huda Hallawi³

¹ Department of Physics, College of Science, University of Babylon, Babel 51001, Iraq

² Through-life Engineering Services Institute, Cranfield Manufacturing, Cranfield University, Cranfield MK43 0AL, UK

³ Department of Information Technology, College of Computer Science and Information Technology, University of Kerbala, Kerbala 56001, Iraq

Corresponding Author Email: sci.wasnaa.jaafar@uobabylon.edu.iq

Copyright: ©2024 The authors. This article is published by IETA and is licensed under the CC BY 4.0 license (<http://creativecommons.org/licenses/by/4.0/>).

<https://doi.org/10.18280/isi.290502>

ABSTRACT

Received: 31 March 2024

Revised: 17 June 2024

Accepted: 10 August 2024

Available online: 24 October 2024

Keywords:

Infrared (IR) thermography measurement, non-destructive testing (NDT), discrete wavelet transform (DWT), spatial resolution enhancement, thermal images

Non-contact infrared thermography measurement has exhibited advantages of cost saving, fast inspection time, and high efficiency. However, infrared thermography has a relatively low spatial resolution which leads to low quality thermal images. This paper suggests a new wavelet-based technique by merging of new edge-directed interpolation (NEDI) with wavelet zero padding (WZP), and discrete wavelet transform (DWT). The developed technique is built upon the target of improving the visual effect of blurring thermal images with increasing spatial resolution, thus producing high quality thermal images. The DWT procedure is applied through dividing the low-resolution image to four frequencies of sub-bands. For a good reconstruction of a high-resolution image, the sub-band of low-frequency is estimated by applying WZP to the perceived image. The rest three sub-bands of high-frequencies are handled by NEDI and a soft threshold-method so as to maintain more edges and remove probable noise. The accomplishment of the suggested approach has been examined on diverse types of thermal images. The experimental results appear the distinction of the suggested technique above the interpolation and state-of-the-art wavelet-based techniques.

1. INTRODUCTION

Primarily, IR thermography is defined as a non-contact temperature measurement based on the emission of infrared radiation of the objects with temperature that is above the absolute zero [1]. The advantages of IR thermography are low cost, high sensitivity, and very fast response and exposure times [2]. IR thermography is split into two categories: Passive and active. The passive approach does not require any external excitation source to measure the temperature of materials under test, which has wide applications on surveillance or condition monitoring, etc. The active approach requires an external thermal excitation source in order to generate a discriminating thermal contrast and both quantitative and qualitative analysis can be applied on the temperature response [3].

IR thermography plays a key role in NDT technology. NDT is a functional technique for revealing, determining, distinguishing, and measuring the inner structure of the materials without rising harm [4]. Contrary to the other NDT techniques, such as Ultrasonic testing and X-ray testing, IR thermography suffers a relatively low spatial resolution which leads to low quality images. Although some thermal image enhancement techniques have been developed, the spatial resolution remains a challenge for industrial applications of thermography [5]. Resolution enhancement has received growing attention and has been employed for several

implementations [6], like thermal imaging [7, 8], satellite imaging [6, 9, 10], medical imaging [11, 12], and video monitoring devices [13], etc.

Spatial resolution indicates to the pixels number for unit area comprised in an image. Resolution enhancement endeavor to recover a high-resolution (HR) image from the perceived low-resolution (LR) image [14]. Employing an elevated-end IR together with an increased spatial resolution is expensive or impracticable owing to an elevated sample average must to be utilized with materials like metals despite they have a high thermal accessibility. Additionally, the border objects or cut out in thermal images is not sharp such the border objects in digital images. This depends on their imaging principals: the digital imaging device is based on the reflected energy by the surface of the observed object with wavelengths in the range of 0.4-0.7 μm , which leads to a high disparity and improved resolution of the acquired digital image. However, the infrared thermal imaging device is depended on reception emitted energy for long wavelengths in the extent of 3-12 μm , which leads to a low contrast and blurring impact of the obtained thermal image because of atmospheric variations and aerosol turbulence [5]. Therefore, the need for an alternative low-cost solution to improve the spatial resolution and create a distinguished contrast without upgrading infrared sensor is highly demanded.

Interpolation is the generally employed image resolution enhancement technique. However, the interpolation methods

such as: bicubic, bilinear, nearest neighbor, and Lanczos are resulted in blurred edges and unwanted artefacts for interpolated images [15]. The wavelet-based resolution enhancement approach has emanated as an active procedure for numerous image processing implementations. The wavelet-domain approaches are eligible to take advantage of the frequency and spatial-domains, and combine merits from both. The appealing attributes, such as multi-resolution for the wavelet transform (WT) cement it to resolve genuine-world signals [16]. The WT divides an image information to sub-bands of low and high- frequencies, and thereafter checks for a resolution coincided to every sub-band scale [17]. The feature for wavelet division is that image attributes are derived from different scales which are separated and resolved: global attributes are tested at rough scales, however local attributes are resolved at soft scales [18].

A few preceding methods have been inserted so as to assess the wavelet coefficients for high-frequency sub-bands. Jin et al. [19] suggested an infrared image enhancement using wavelet transform based on applying different filtering coefficients toward different directions. They performed directional smoothing over the tangential orientation of edge in order to amend its continuity, while directional sharpening over the normal orientation in order to upgrade the disparity. Gao et al. [20] proposed a nonlinear method for enhancing infrared images using discrete stationary wavelet transform and contrast limited adaptive histogram equalization (CLAHE) to address the problem of low contrast and low resolution, blurring edge and noise for infrared images. In the study by Binbin [21], a denoising method for infrared images is presented, which uses the thresholding of wavelet coefficients. This method is depended on the features of noise allocation for infrared images, and the wavelet coefficients of the transformed image for denoising the image. However, the relatively low spatial resolution of thermal images remains a challenge for industrial applications of IR thermography.

This paper suggests an image amended approach based on a combination of three methods namely: WZP, and NEDI as well as DWT. The motivation of this paper is to boost the spatial resolution and contrast, and retrieve the sharp edges for degraded thermal images of IR thermography.

The deficiencies in thermal images are summarized via a minimum spatial resolution owing to the thermal sensor which restricts the measurements precision and reliability for IR thermography. Additionally, the border of objects at thermal images is not acute which leads to low contrast and blurred edges. Moreover, the noise artefacts resulted from recorded images by infrared sensors which add additional blurring. The paper is regulated as follows. Section 2 offered the developed method. Results and discussions using five thermal images were displayed at Section 3, and conclusions were exhibited at Section 4.

2. THE ENHANCEMENT RESOLUTION TECHNIQUE

Preserving the high-frequencies (e.g. edges) for the noticed LR image is the major objective for resolution enhancing techniques. In this research, the DWT operation is applied to insulate and maintain the edges components of the LR image, and thereafter the up-scaling of insulate components at the sub-bands of high-frequencies is applied. The idea is that employing the interpolation of insulate components will maintain preferable edges for the image in comparison to

employing an immediate interpolation that degrades the edges. A few methods based on DWT, which include DWT [22], DASR [23], DWT-Dif [24], DWT-SWT [25], have been evolved to maintain the edges at the interpolated sub-bands. However, the possible wastage of edges is increased in these sub-bands because of the degradation impact from their applied interpolation methods. Therefore, NEDI [26] technique is applied to combine with DWT, as suggested in our previous approach, called DWT-NEDI [6] technique to best maintain the edges for interpolated sub-bands.

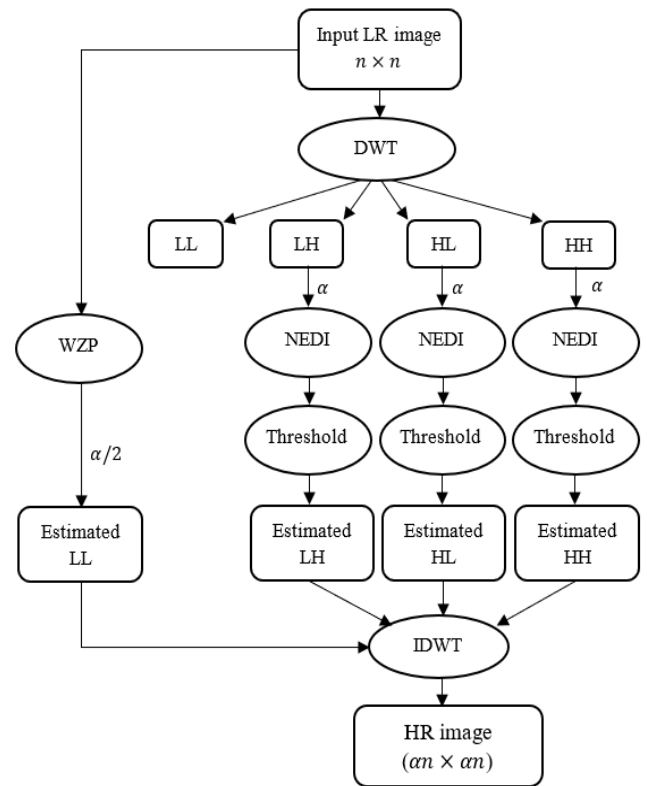


Figure 1. The graph of the proposed resolution enhancement technique

This paper suggests to employ a collection of WZP [27] method and the so-called DWT-NEDI approach to boost the resolution and retrieve the wasted edges for low quality thermal images. The principal concept of each method is that the DWT [6] is a process of dividing the treated image into quadrable sub-bands of frequencies; accomplished by dilations and translations using the mother wavelet function. Due to the down-sampling process that utilized by the DWT, thereby every sub-band reduces to half size. The fundamental concept of NEDI [26] is assessing new points by computing a weighted average of the four nearest neighbour points over the diagonal orientations. The concept of WZP [27] is represented by exchanging low-frequency sub-band by perceived image, whereas the high-frequencies are fulfilled for zeros. Firstly, each level of DWT operation separates the input image to quadric sub-bands of low and high (LL, LH, HL, and HH). Secondly, the LL sub-band is replaced by the output of WZP method on the LR image for the up-sample factor $\alpha/2$. The rest high frequencies of LH, HL, and HH are up sampled by applying NEDI technique for the up-sample factor α . Image information registered by infrared systems are become spoiled by an additive noise, thus, to maintain extra details and eliminate noise at the processed images, a soft-threshold

method [28, 29] is employed. The threshold τ for the considered sub-band is computed by:

$$\tau = \sigma\sqrt{2 \log(N) / N} \quad (1)$$

whereas σ and N mean the standard deviation and the aggregate pixel numbers respectively. The function of soft-threshold can be defined as below:

$$X_{out}(i, j) = \begin{cases} X_{in}(i, j) - \tau & X_{in}(i, j) > \tau \\ 0 & |X_{in}(i, j)| \leq \tau \\ X_{in}(i, j) + \tau & X_{in}(i, j) < -\tau \end{cases} \quad (2)$$

Soft-threshold heads for preserving signal larger coefficients and minifying noise coefficients to zero. Finally, IDWT operation is employed for performing the improved image resolution by joining the assessed LL, LH, HL, and HH. The graph of the proposed technique is clarified via Figure 1. The specific processing steps and parameter selections can be described by

- (1) Considering the red component from the input image.
- (2) Applying the DWT operation with one-level to separate this component to four frequencies of sub-bands.
- (3) Applying the NEDI method for the up-sample factor α related to up-sample frequencies of LH, HL, and HH
- (4) After computing threshold τ for each sub-band, the soft-thresholding should be employed to generate the assessed LH, HL, and HH.
- (5) Applying WZP method for the up-sample factor $\alpha/2$ to up-sample the LR image for generating the assessed LL of low-frequency.
- (6) Applying the IDWT operation to combine all these

processed sub-bands for obtaining the improved channel.

(7) In regards to the blue and green components repeat step 2 to 7.

(8) The amended HR colour image is produced by merging the three processed components.

3. RESULTS AND DISCUSSIONS

3.1 Assessment of visual performance

This part demonstrates the empirical results of visual performance assessment for testing the suggested method and other considered resolution enhancement methods on thermal images. The implemented technique was examined on five thermal images *Woman, Hands, Legs, CFC panel* and *Truck axle* for performance evaluation in terms of several kinds of images. The intrinsic relationship between the adopted thermal images is that these images with various features and for diverse applications. The original HR images come with variable scales; therefore, they were rescaled to 512×512 pixels and considered the row images. Additionally, the blurring and down-sampling were applied to the row of HR image, in order to create the scale of 128×128 . They were carried by employing two times DWT of wavelet dB.9/7 function. In other words, the LR image is considered as the LL sub-band of the second-level DWT of the row HR image. This LR image was more contaminated using a white Gaussian noise of 40 dB SNR (Signal-to-Noise Ratio). Based on literature survey, the Daubechies of (dB.9/7) has been adopted as it is the best ordinarily employed wavelet function of the separating operation by DWT for resolution enhancement and it can also eliminate the problem of border artefacts [30].

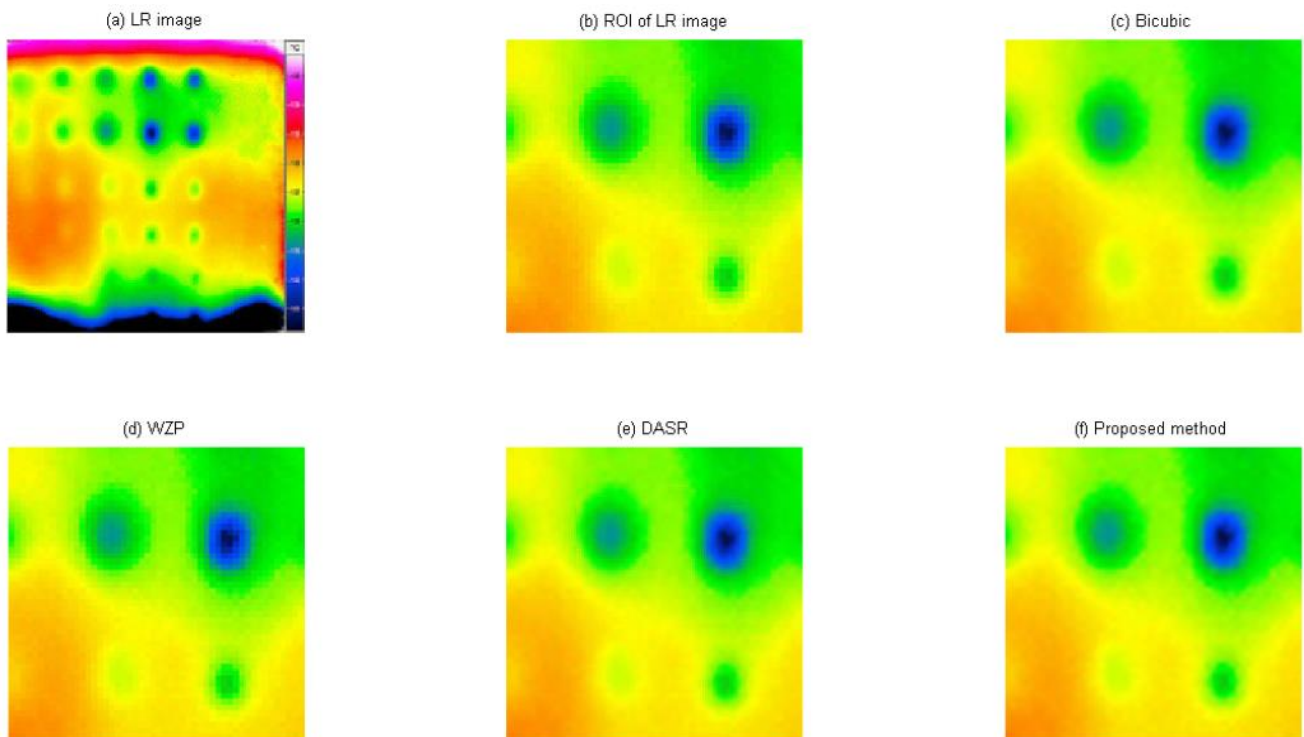


Figure 2. Images with improved resolution outcome of the suggested technique with up-sampling of " 128×128 " to " 512×512 " of the CFC plate image. (a) LR complete image; (b) Partial LR image; the improved images are depicted in (c), (d), (e) and (f) which stands for Bicubic, WZP, DASR and the new proposed technique respectively

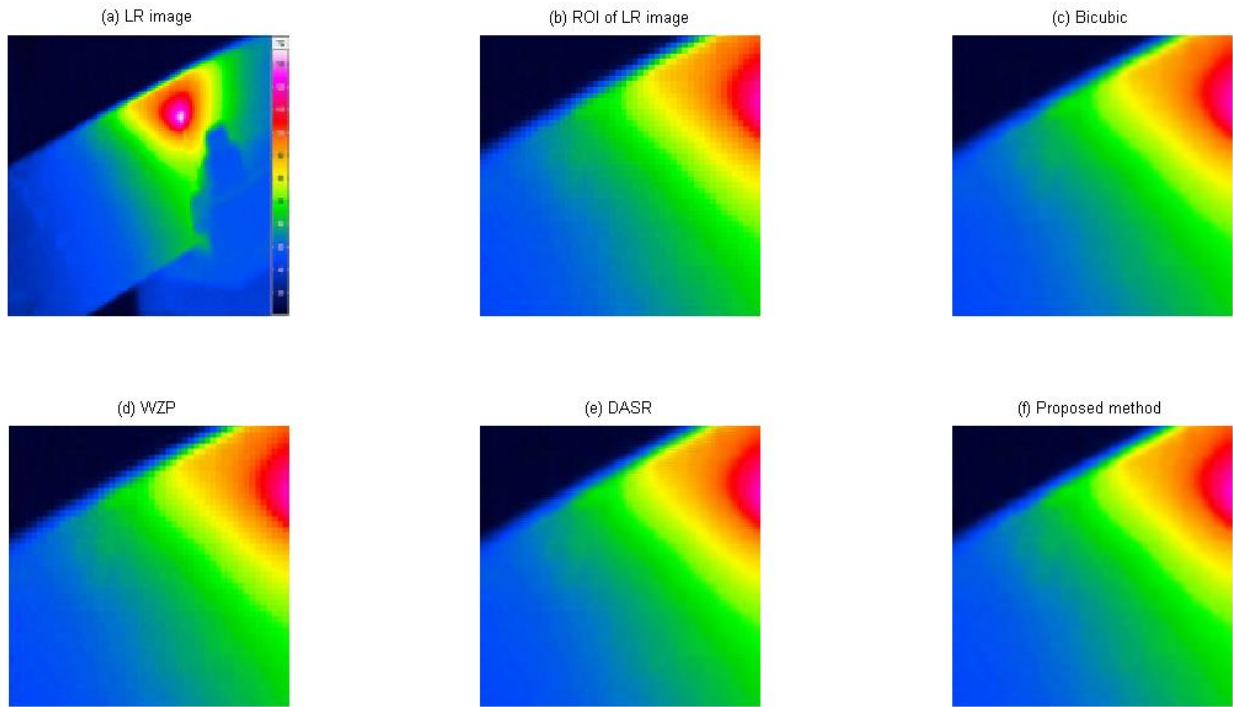


Figure 3. Images with improved resolution outcome of the suggested technique with up-sampling of " 128×128 " to " 512×512 " of the truck axle image. (a) LR complete image; (b) Partial LR image; the improved images are depicted in (c), (d), (e) and (f) which stands for Bicubic, WZP, DASR, and the new proposed technique respectively

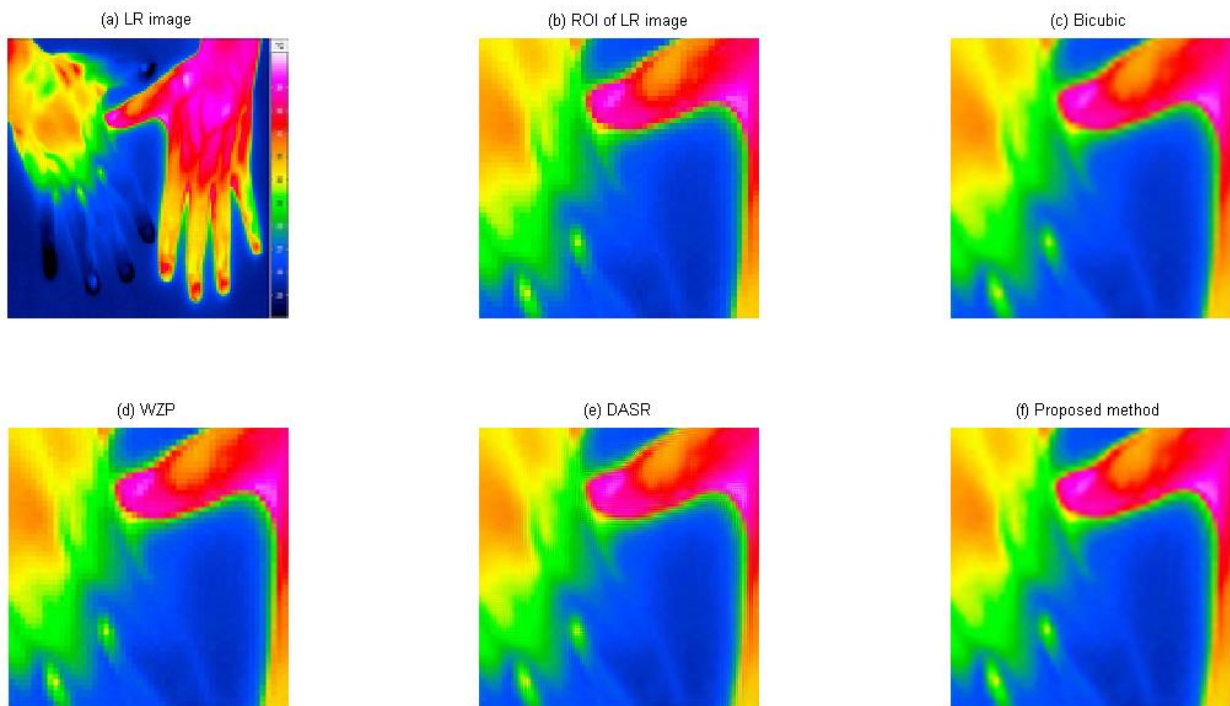


Figure 4. Images with improved resolution outcome of the suggested technique with up-sampling of " 128×128 " to " 512×512 " of Hand image. (a) LR complete image; (b) Partial LR image; whereas the enhanced images are showed in (c), (d), (e) and (f) which stands for Bicubic, WZP, DASR, and the new technique respectively

To present the visual results, three images were adopted from the five thermal images and examined by the suggested technique. Figures 2-4 demonstrate the improved images by the suggested technique and the other studied techniques for an up-sampling from 128×128 pixels to 512×512 pixels of the three selected images. It is viewed from the visual results that the suggested technique has the ability to upgrade the acquired LR images by proving more edge details of interested areas. It

has also the capability to enhance the contrast and significantly amend the visual effect for the observed images. For example, the edges of CFC plate and Truck axle images resulted from the suggested method are extremely immaculate, and the border of objects of interested areas in these images is distinguished clearly, in comparison to the images obtained by the other techniques. Identical visible outcomes were noticed from other examined images. Noise and aliasing effects were

compressed by the suggested algorithm. The aliasing effects of Hand image, for instance, are suppressed obviously by the proposed method, while these effects are exhibited distinctly in the images resulted from the other methods.

3.2 Assessment of quantitative performance

The distinction between the resolution improved images of several methods is tiny and it is complicated to be checked visually. This part displays the experimental values of objective performance evaluation. Peak-signal-to-noise-ratio (PSNR) was used to evaluate image quality, because it has been known as the most important and ordinarily employed quantitative measure; it was applied to quantify the ratio between the resultant and the row HR images. It can be computed as below:

$$PSNR = 10 \log_{10} \left(\frac{L^2}{MSE} \right) \quad (3)$$

where, L means the top value at the image. Within grayscale symbolized image of 8-bit, the L amount equals to 255. Mean-Square-Error (MSE) was used to convey the ratio of the improved $\hat{X}(i, j)$ and the row HR $X(i, j)$ images. MSE is computed by:

$$MSE = \frac{1}{W \times H} \sum_{i=1}^W \sum_{j=1}^H [\hat{X}(i, j) - X(i, j)]^2 \quad (4)$$

The root-mean-square error (RMSE) is as well one of the generally employed objective measures [31], and it computed as:

$$RMSE = \sqrt{MSE} \quad (5)$$

Entropy is also employed to appreciate quantitatively image performance when the mistake of images for various image upgraded approaches are much relative to every other and it is quite complicated to do appreciation. The entropy for a negative mistake of image, called by E , is computed by

$$E = - \sum_{k=1}^L P(r_k) \log_2 P(r_k) \quad (6)$$

where, $P(r_k)$ means the prospect of a brightness value r_k . The study by Wang et al. [32] shows the best refinement with the minimal E .

Tables 1-3 display the objective results achieved through PSNR, RMSE, and Entropy analysis for selected thermal images. According to the PSNR and RMSE values, the proposed method outperforms the others across all five tested images. Figure 5 presents a comparative analysis of PSNR, RMSE, and Entropy for all evaluated images. The results indicate that the adopted method achieves the highest PSNR and RMSE values (42.20 dB, 25.32 dB, 26.57 dB, 29.10 dB, and 29.83 for PSNR; 1.89, 13.81, 11.97, 8.94, and 9.02 for RMSE) for each of the five images, respectively, showing improvements of 5%, 1%, 2%, 7%, and 5% over the DWT-NEDI method, respectively. In terms of Entropy, the DWT-NEDI method performs better for the Woman, Legs, CFC panel, and Truck axle images, while the proposed method excels for the Hand image. These findings suggest that the effectiveness of the evaluated techniques varies depending on the specific characteristics of the images and the metrics used for performance evaluation.

Table 1. Results of PSNR (dB) with thermal images and improved resolution of 128×128 to 512×512

Techniques	Image Type				
	Woman	Hands	Legs	CFC	Truck
Nearest	32.25	23.51	24.46	26.60	27.12
Bilinear	33.90	23.84	24.93	27.42	27.67
Bicubic	33.88	23.87	24.91	27.41	27.69
Lanczos	33.82	23.82	24.86	27.36	27.68
WZP [27]	34.74	24.35	25.33	27.68	27.87
DWT [23]	34.66	24.29	25.29	27.58	27.81
DASR [24]	35.55	24.00	25.28	27.09	27.65
DWT-Dif [25]	31.94	22.78	24.08	25.75	26.40
DWT-SWT [26]	32.55	23.40	24.39	26.19	26.90
DWT-NEDI [6]	40.19	25.02	26.13	27.27	27.74
Proposed method	42.20	25.32	26.57	29.10	29.03

Table 2. Results of RMSE with the thermal images and improved resolution of 128×128 to 512×512

Techniques	Image Type				
	Woman	Hands	Legs	CFC	Truck
Nearest	6.23	17.02	15.26	11.93	11.23
Bilinear	5.15	16.40	14.46	10.85	10.55
Bicubic	5.16	16.33	14.49	10.87	10.52
Lanczos	5.19	16.42	14.58	10.92	10.54
WZP [27]	4.68	15.46	13.81	10.53	10.30
DWT [23]	4.72	15.57	13.87	10.65	10.38
DASR [24]	4.26	16.09	13.89	11.28	10.57
DWT-Dif [25]	6.45	18.51	15.96	13.16	12.20
DWT-SWT [26]	6.01	17.24	15.39	12.51	11.53
DWT-NEDI [6]	2.50	14.31	12.59	11.04	10.46
Proposed method	1.89	13.81	11.97	8.94	9.02

Table 3. Outcomes of entropy with picked thermal images and improved resolution of 128×128 to 512×512

Techniques	Image Type				
	Woman	Hands	Legs	CFC	Truck
Nearest	5.21	4.32	3.58	3.85	3.22
Bilinear	5.79	4.25	3.58	3.69	3.11
Bicubic	5.84	4.27	3.60	3.73	3.13
Lanczos	5.91	4.32	3.65	3.77	3.18
WZP [27]	5.30	4.13	3.51	3.64	3.04
DWT [23]	5.22	4.15	3.54	3.66	3.07
DASR [24]	5.36	4.19	3.46	3.58	3.06
DWT-Dif [25]	5.36	4.29	3.70	3.56	2.92
DWT-SWT [26]	4.75	4.04	3.54	3.68	3.03
DWT-NEDI [6]	4.57	3.73	3.13	3.10	2.62
Proposed method	4.99	3.67	3.16	3.17	2.89

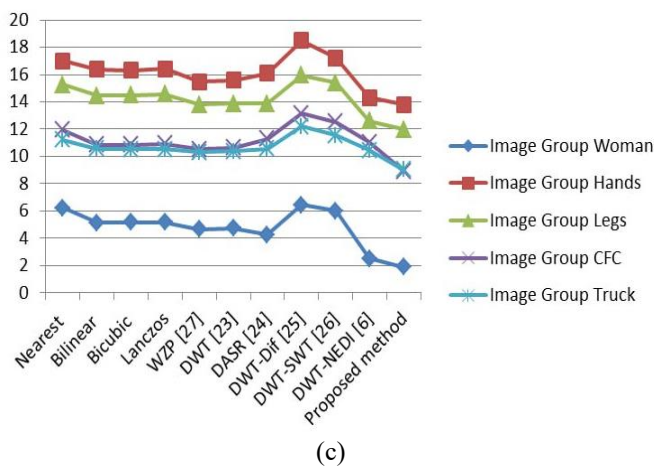
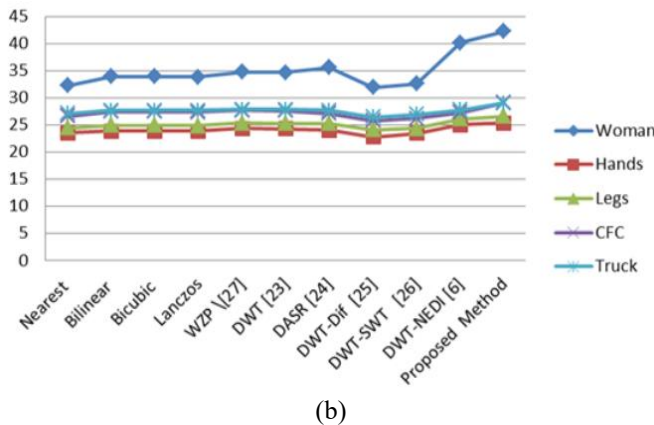
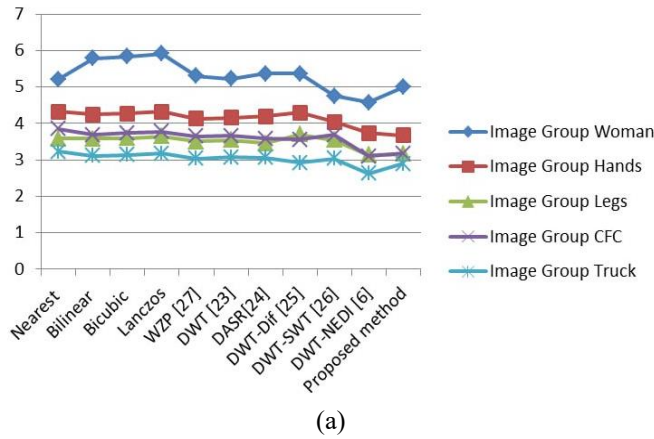


Figure 5. Comparison of PSNR, RMSE, and entropy results for tested images utilizing the suggested approach and wavelet-based interpolation techniques

3.3 Assessment of wavelet functions performance

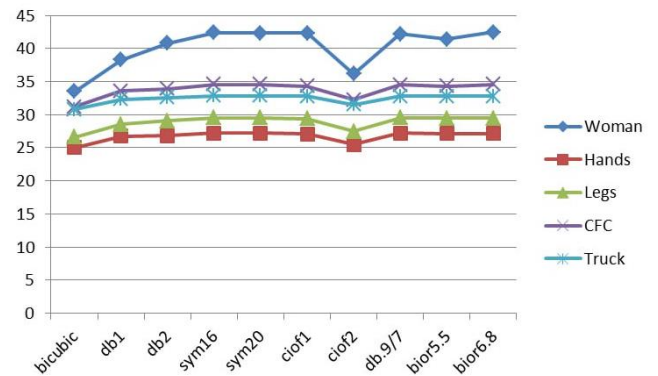


Figure 6. Comparison of PSNR results for the selected images using different wavelet functions

Table 4. PSNR values for five thermal images using selected high-performance wavelet functions, highlighting top five results

Wavelet Functions	Woman	Hands	Legs	CFC	Truck
bicubic	33.54	25.04	26.60	31.18	30.77
dB1	38.32	26.73	28.54	33.56	32.32
dB2	40.84	26.79	29.08	33.94	32.58
sym16	42.37	27.21	29.55	34.55	32.83
sym20	42.33	27.20	29.55	34.55	32.83
ciof1	42.30	27.11	29.40	34.33	32.80
ciof2	36.17	25.47	27.50	32.29	31.51
dB9/7	42.22	27.19	29.51	34.48	32.82
bior5.5	41.41	27.14	29.49	34.31	32.76
bior6.8	42.44	27.18	29.50	34.55	32.82

The suggested approach, along with other studied techniques, was implemented using the optimal wavelet filter dB.9/7. This section explores the feasibility of employing the suggested DWT-NEDI-WZP method with alternative wavelet functions for five thermal images. Our previous research [33] demonstrates that choosing the wavelet function plays a crucial part in enhancing achievement. An aggregate of 50 wavelet functions, encompassing sym.2-20, coef.1-5, dB.1-20, and bior.1-6 [34], were evaluated using the DWT-NEDI-WZP approach. Table 4 presents the PSNR results for selected thermal images using nine wavelet filters—ciof1, ciof2, dB1, dB2, dB9/7, sym16, sym20, bior5.5, and bior6.8—which were chosen due to their superior performance compared to other wavelet functions. Figure 6 illustrates a comparison of the PSNR results for the tested images using these nine wavelet

functions. From Figure 6, it can be inferred that the proposed approach performs well with various functions other than dB.9/7. According to the PSNR outcomes, the top-performing wavelet functions are sym20, sym16, bior6.8, bior5.5, and coif1, although the differences among them are not distinctive.

4. CONCLUSIONS

A new resolution enhancement approach resulted from special integration of WZP, and DWT and NEDI was suggested in this research to generate a high contrast and recover image details for different types of acquired low quality thermal images. To best look after the sharp details and eliminate noise in the processed images, a soft threshold method is also employed. The developing of this approach is not only to protect extra edges and suppress the noise caused by infrared sensors, but also enhance the contrast and significantly improve visual effect of degraded thermal images for industrial applications of IR thermography. Five different types of thermal images were tested by the suggested technique and compared with other state-of-the-art wavelet-based methods. Experimental results appear that the suggested technique performs better than other studied techniques in both visual and quantitative terms.

However, there was a limitation of the process to generate the perceived LR image for the proposed approach. However, there is no validated model which could completely explore this subordinate process.

ACKNOWLEDGMENT

We would like to express our deep gratitude to the Iraqi Ministry of Higher Education and Scientific Research for their continued support and encouragement. We offer our sincere appreciation for the learning opportunities provided by our ministry.

REFERENCES

- [1] de Jesus Guirro, R.R., Oliveira Lima Leite Vaz, M.M., das Neves, L.M.S., Dibai-Filho, A.V., Carrara, H.H.A., de Oliveira Guirro, E.C. (2017). Accuracy and reliability of infrared thermography in assessment of the breasts of women affected by cancer. *Journal of Medical Systems*, 41: 87. <https://doi.org/10.1007/s10916-017-0730-7>
- [2] Optris, G. (2019). Basic principles of non-contact temperature measurement. *Innovation Infrared Technology*, 1: 39.
- [3] Zhang, H., Yang, R., He, Y., Foudazi, A., Cheng, L., Tian, G. (2017). A review of microwave thermography nondestructive testing and evaluation. *Sensors*, 17(5): 1123. <https://doi.org/10.3390/s17051123>
- [4] Du, W., Zhao, Y., Roy, R., Addepalli, S., Tinsley, L. (2018). A review of miniaturised Non-Destructive Testing technologies for in-situ inspections. *Procedia Manufacturing*, 16: 16-23. <https://doi.org/10.1016/j.promfg.2018.10.152>
- [5] Du, W., Addepalli, S., Zhao, Y. (2019). The spatial resolution enhancement for a thermogram enabled by controlled subpixel movements. *IEEE Transactions on Instrumentation and Measurement*, 69(6): 3566-3575. <https://doi.org/10.1109/TIM.2019.2932175>
- [6] Witwit, W., Zhao, Y., Jenkins, K., Zhao, Y. (2017). Satellite image resolution enhancement using discrete wavelet transform and new edge-directed interpolation. *Journal of Electronic Imaging*, 26(2): 023014. <https://doi.org/10.1117/1.JEI.26.2.023014>
- [7] Holland, S.D., Renshaw, J. (2010). Physics-based image enhancement for infrared thermography. *NDT & E International*, 43(5): 440-445. <https://doi.org/10.1016/j.ndteint.2010.04.004>
- [8] Ashiba, H.I., Mansour, H.M., El-Kordy, M.F., Ahmed, H.M. (2015). A new approach for contrast enhancement of infrared images based on contrast limited adaptive histogram equalization. *Applied Mathematics & Information Sciences Letters*, 3(3): 123-125. <https://doi.org/10.12785/amisl/030306>
- [9] Demirel, H., Anbarjafari, G. (2009). Satellite image resolution enhancement using complex wavelet transform. *IEEE Geoscience and Remote Sensing Letters*, 7(1): 123-126. <https://doi.org/10.1109/LGRS.2009.2028440>
- [10] Iqbal, M.Z., Ghafoor, A., Siddiqui, A.M. (2012). Satellite image resolution enhancement using dual-tree complex wavelet transform and nonlocal means. *IEEE Geoscience and Remote Sensing Letters*, 10(3): 451-455. <https://doi.org/10.1109/LGRS.2012.2208616>
- [11] Robinson, M.D., Chiu, S.J., Toth, C.A., Izatt, J.A., Lo, J.Y., Farsiu, S. (2017). New applications of super-resolution in medical imaging. In *Super-Resolution Imaging*, pp. 383-412. <https://doi.org/10.1201/9781439819319>
- [12] Greenspan, H. (2009). Super-resolution in medical imaging. *The Computer Journal*, 52(1): 43-63. <https://doi.org/10.1093/comjnl/bxm075>
- [13] Zhang, L., Zhang, H., Shen, H., Li, P. (2010). A super-resolution reconstruction algorithm for surveillance images. *Signal Processing*, 90(3): 848-859. <https://doi.org/10.1016/j.sigpro.2009.09.002>
- [14] Park, S.C., Park, M.K., Kang, M.G. (2003). Super-resolution image reconstruction: A technical overview. *IEEE Signal Processing Magazine*, 20(3): 21-36. <https://doi.org/10.1109/MSP.2003.1203207>
- [15] Pratt, W.K. (2007). *Digital Image Processing: PIKS Scientific Inside*. WILEY Online Library. <https://doi.org/10.1002/0470097434>
- [16] Crouse, M.S., Nowak, R.D., Baraniuk, R.G. (1998). Wavelet-based statistical signal processing using hidden Markov models. *IEEE Transactions on signal processing*, 46(4): 886-902. <https://doi.org/10.1109/78.668544>
- [17] Daubechies, I. (1992). *Ten Lectures on Wavelets*. Society for Industrial and Applied Mathematics. CBMS-NSF Regional Conference Series in Applied Mathematics. <https://doi.org/10.1137/1.9781611970104>
- [18] Nguyen, N., Milanfar, P. (2000). A wavelet-based interpolation-restoration method for superresolution (wavelet superresolution). *Circuits, Systems and Signal Processing*, 19: 321-338. <https://doi.org/10.1007/BF01200891>
- [19] Jin, H.B., Fan, C.X., Wang, Q.Y., Li, Y. (2017). Improvement of infrared image based on directional anisotropic wavelet transform. *Electronic Imaging*, 29: 51-55. <https://doi.org/10.2352/ISSN.2470-1173.2017.2.VIPC-406>

- [20] Gao, C., Yun, L., Wang, K., Ye, Z., Li, H. (2019). Infrared image enhancement method based on discrete stationary wavelet transform and CLAHE. In 2019 IEEE International Conference on Computer Science and Educational Informatization (CSEI), Kunming, China, pp. 191-194. <https://doi.org/10.1109/CSEI47661.2019.8938871>
- [21] Binbin, Y. (2019). An improved infrared image processing method based on adaptive threshold denoising. *EURASIP Journal on Image and Video Processing*, 2019(1): 5. <https://doi.org/10.1186/s13640-018-0401-8>
- [22] Tsai, P.S., Acharya, T., (2006). Image processing up-sampling using discrete wavelet transform. In *Proceedings of the 9th Joint International Conference on Information Sciences (JCIS-06)*. <https://doi.org/10.2991/jcis.2006.340>
- [23] Anbarjafari, G., Demirel, H. (2010). Image super resolution based on interpolation of wavelet domain high frequency subbands and the spatial domain input image. *ETRI Journal*, 32(3): 390-394. <https://doi.org/10.4218/etrij.10.0109.0303>
- [24] Demirel, H., Anbarjafari, G. (2011). Discrete wavelet transform-based satellite image resolution enhancement. *IEEE Transactions on Geoscience and Remote Sensing*, 49(6): 1997-2004. <https://doi.org/10.1109/TGRS.2010.2100401>
- [25] Demirel, H., Anbarjafari, G. (2010). Image resolution enhancement by using discrete and stationary wavelet decomposition. *IEEE Transactions on Image Processing*, 20(5): 1458-1460. <https://doi.org/10.1109/TIP.2010.2087767>
- [26] Li, X., Orchard, M. T. (2001). New edge-directed interpolation. *IEEE Transactions on Image Processing*, 10(10): 1521-1527. <https://doi.org/10.1109/83.951537>
- [27] Temizel, A., Vlachos, T. (2005). Wavelet domain image resolution enhancement using cycle-spinning. *Electronics Letters*, 41(3): 1.
- [28] Donoho, D.L. (1995). De-noising by soft-thresholding. *IEEE Transactions on Information Theory*, 41(3): 613-627. <https://doi.org/10.1109/18.382009>
- [29] Zhang, X.P. (2001). Thresholding neural network for adaptive noise reduction. *IEEE Transactions on Neural Networks*, 12(3): 567-584. <https://doi.org/10.1109/72.925559>
- [30] Skodras, A., Christopoulos, C., Ebrahimi, T. (2001). The JPEG 2000 still image compression standard. *IEEE Signal Processing Magazine*, 18(5): 36-58. <https://doi.org/10.1109/79.952804>
- [31] Azam, S., Zohra, F.T., Islam, M.M. (2014). A state-of-the-art review on wavelet based image resolution enhancement techniques: performance evaluation criteria and issues. *International Journal of Image, Graphics and Signal Processing*, 6(9): 346. <https://doi.org/10.5815/ijigsp.2014.09.05>
- [32] Wang, Z., Bovik, A.C., Sheikh, H.R., Simoncelli, E.P. (2004). Image quality assessment: from error visibility to structural similarity. *IEEE Transactions on Image Processing*, 13(4): 600-612. <https://doi.org/10.1109/TIP.2003.819861>
- [33] Witwit, W., Zhao, Y., Jenkins, K.W., Zhao, Y. (2016). An optimal factor analysis approach to improve the wavelet-based image resolution enhancement techniques. *Global Journal of Computer Science and Technology*, 16(3).
- [34] Qidwai, U., Chen, C.H. (2009). *Digital image processing: An algorithmic approach with MATLAB*. Chapman and Hall/CRC, New York. <https://doi.org/10.1201/9781420079517>